NASA/TP-2008-214771

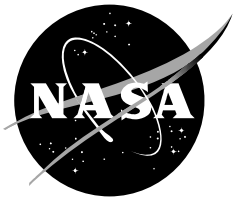

Three-Dimensionally Engineered Normal Human Lung Tissue-Like Assemblies: Target Tissues for Human Respiratory Viral Infections

*Thomas J. Goodwin, Ph.D.**[1]
M. McCarthy, B.S.[2]
Y-H. Lin, Ph.D.[3]
A.M Deatly, Ph.D. [3]

[1]*Disease Modelling/Tissue Analogues Laboratory*
NASA Johnson Space Center
2101 NASA Parkway, Houston, Texas 77058

[2]*Universities Space Research Association*
Division of Space Life Sciences
3600 Bay Area Boulevard
Houston TX 77058

[3]*Vaccines Discovery*
Wyeth Research
401 N. Middletown Rd
Pearl River, New York 10965

**To whom requests for reprints should be addressed at NASA Johnson Space Center*

March 2008

THE NASA STI PROGRAM OFFICE . . . IN PROFILE

Since its founding, NASA has been dedicated to the advancement of aeronautics and space science. The NASA Scientific and Technical Information (STI) Program Office plays a key part in helping NASA maintain this important role.

The NASA STI Program Office is operated by Langley Research Center, the lead center for NASA's scientific and technical information. The NASA STI Program Office provides access to the NASA STI Database, the largest collection of aeronautical and space science STI in the world. The Program Office is also NASA's institutional mechanism for disseminating the results of its research and development activities. These results are published by NASA in the NASA STI Report Series, which includes the following report types:

- TECHNICAL PUBLICATION. Reports of completed research or a major significant phase of research that present the results of NASA programs and include extensive data or theoretical analysis. Includes compilations of significant scientific and technical data and information deemed to be of continuing reference value. NASA's counterpart of peer-reviewed formal professional papers but has less stringent limitations on manuscript length and extent of graphic presentations.

- TECHNICAL MEMORANDUM. Scientific and technical findings that are preliminary or of specialized interest, e.g., quick release reports, working papers, and bibliographies that contain minimal annotation. Does not contain extensive analysis.

- CONTRACTOR REPORT. Scientific and technical findings by NASA-sponsored contractors and grantees.

- CONFERENCE PUBLICATION. Collected papers from scientific and technical conferences, symposia, seminars, or other meetings sponsored or cosponsored by NASA.

- SPECIAL PUBLICATION. Scientific, technical, or historical information from NASA programs, projects, and mission, often concerned with subjects having substantial public interest.

- TECHNICAL TRANSLATION. English-language translations of foreign scientific and technical material pertinent to NASA's mission.

Specialized services that complement the STI Program Office's diverse offerings include creating custom thesauri, building customized databases, organizing and publishing research results . . . even providing videos.

For more information about the NASA STI Program Office, see the following:

- Access the NASA STI Program Home Page at http://www.sti.nasa.gov

- E-mail your question via the internet to help@sti.nasa.gov

- Fax your question to the NASA Access Help Desk at (301) 621-0134

- Telephone the NASA Access Help Desk at (301) 621-0390

- Write to:
  NASA Access Help Desk
  NASA Center for AeroSpace Information
  7115 Standard
  Hanover, MD 21076-1320

NASA/TP-2008-214771

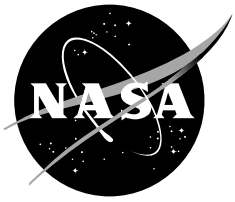

Three-Dimensionally Engineered Normal Human Lung Tissue-Like Assemblies: Target Tissues for Human Respiratory Viral Infections

*Thomas J. Goodwin, Ph.D.**[1]
M. McCarthy, B.S.[2]
Y-H. Lin, Ph.D.[3]
A.M Deatly, Ph.D. [3]

[1]*Disease Modelling/Tissue Analogues Laboratory*
NASA Johnson Space Center
2101 NASA Parkway, Houston, Texas 77058

[2]*Universities Space Research Association*
Division of Space Life Sciences
3600 Bay Area Boulevard
Houston TX 77058

[3]*Vaccines Discovery*
Wyeth Research
401 N. Middletown Rd
Pearl River, New York 10965

**To whom requests for reprints should be addressed at NASA Johnson Space Center.*

March 2008

Available from:

NASA Center for AeroSpace Information
7115 Standard Drive
Hanover, MD 21076-1320
301-621-0390

National Technical Information Service
5285 Port Royal Road
Springfield, VA 22161
703-605-6000

This report is also available in electronic form at http://ston.jsc.nasa.gov/collections/TRS/

Contents

Tables

Figures

Acronyms

2D	two-dimensional
3D	three-dimensional
ALI	air liquid interface
BEAS-2B	human bronchial epithelial immortalized cell line
BV	budding virus
CMF-PBS	calcium- and magnesium-free phosphate-buffered saline
CO_2	carbon dioxide
EtOH	ethanol
FBS	fetal bovine serum
H&E	haematoxylin and eosin
HBE	human bronchial epithelial
HBTC	human mesenchymal bronchial-tracheal cells
HIV	human immunodeficiency virus
IHC	immunohistochemistry
MOI	multiplicity of infection
MV	microvilli
PBS	phosphate-buffered saline
pi	post infection
RWV	rotating cylindrical tissue culture vessels
SEM	scanning electron microscopy
TEM	transmission electron microscopy
TJ	tight junctions
TLA	(three-dimensional human lung epithelio-mesenchymal) tissue-like assemblies
VNC	viral nucleocapsids

Abstract

In vitro three-dimensional (3D) human lung epithelio-mesenchymal tissue-like assemblies (3D hLEM TLAs), from this point forward referred to as TLAs, were engineered in rotating wall vessel technology to mimic the characteristics of *in vivo* tissues, thus providing a tool to study human respiratory viruses and host cell and viral interactions. The TLAs were bioengineered onto collagen-coated cyclodextran microcarriers using primary human mesenchymal bronchial-tracheal cells as the foundation matrix and an adult human bronchial epithelial immortalized cell line as the overlying component. The resulting TLAs share significant characteristics with *in vivo* human respiratory epithelium including polarization, tight junctions, desmosomes, and microvilli. The presence of tissue-like differentiation markers including villin, keratins, and specific lung epithelium markers, as well as the production of tissue mucin, further confirm that these TLAs differentiated into tissues functionally similar to *in vivo* tissues. Increasing virus titers for human respiratory syncytial virus and the detection of membrane bound glycoproteins over time confirm productive infection with the virus. Therefore, we assert TLAs mimic aspects of the human respiratory epithelium and provide a unique capability to study the interactions of respiratory viruses and their primary target tissue independent of the host's immune system.

1.0 Introduction

The function of respiratory epithelium is critical in protecting humans from disease and acts as a barrier to invading microbes present in the air, defending the host through a complex multilayered system.[1] This complex system is comprised of pseudo-stratified epithelial cells, a basement membrane, and underlying mesenchymal cells. Ciliated, secretory, and basal epithelial cells are joined by intercellular junctions and anchored to the basement membrane via desmosomal interactions. Through tight junctions and the mucociliary layer, the basement membrane maintains polarity of the epithelium and presents a physical barrier between the mesenchymal layer and the airway.[2,3]

Airway epithelial cells defend the host physiology blocking paracellular permeability, modulating airway function through cellular interactions and transporting inhaled microorganisms away via ciliated epithelial cells.[4,5] Epithelial cells, which are regulators of the innate immune response, also induce potent immunomodulatory and inflammatory mediators (cytokines and chemokines) recruiting phagocytic and inflammatory cells, thus facilitating microbial destruction.[6,7,3,2]

Optimally, a cell-based model should reproduce the structural organization, multicellular complexity, differentiation state, and function of the human respiratory epithelium. Immortalized human epithelial cell lines (two-dimensional [2D]), (i.e., BEAS-2B),[8] primary normal human bronchial epithelial (HBE) cells (2D),[9] and air-liquid interface cultures (three-dimensional [3D])[10] are used to study respiratory virus infections *in vitro*. Traditional monolayer cultures of human immortalized and tumor alveolar and broncho-epithelial cells represent homogenous lineages; however, when propagated as 2D cultures, such cultures fail to express the innate tissue fidelity characteristic of normal human respiratory epithelia.[11] Thus, their state of differentiation and intracellular signaling pathways differ from epithelial cells *in vivo*. Primary isolates of HBE cells provide a pseudo-differentiated model with structure and function similar to epithelial cells *in vivo*; this fidelity is short-lived *in vitro*.[9,12] Air-liquid interface cultures of primary HBE cells (or submerged cultures of human adenoid epithelial cells)[13] are grown on collagen-coated filters in wells, on top of a permeable filter. These cells receive nutrients basolaterally and their apical side is exposed to humidified air. The result is a culture of well-differentiated heterogeneous (ciliated, secretory, basal) epithelial cells that are essentially identical to airway epithelium in situ.[14,10,15] Although this model mimics fidelity to the human respiratory epithelium in structure and function, maintenance of consistent cultures is difficult, time consuming, and restricted to small-scale production, thereby limiting industrial pharmaceutical research capability.

Thus, cellular differentiation involves complex cellular interactions[16,17,18] in which cell membrane junctions, extracellular matrices (e.g., basement membrane and ground substances), and soluble signals (endocrine, autocrine, and paracrine) play sustaining roles[19,20,21,22] in tissue development. This process is also influenced by spatial cellular relationships to one another. Each HBE cell has three membrane surfaces: a free-apical surface, a lateral surface, and a basal surface that interacts with mesenchymal cells.[23] Therefore, complex recapitulated 3D models must emulate these characteristics.

In the absence of a reproducible long-term methodology to culture human respiratory epithelium (>3 mm diameter), an established technology developed at NASA's Johnson Space Center is now being used to construct large-scale, 3D, *in vitro* tissue models of human respiratory epithelium (figure 1) and many other tissues[24,25,26] (Table I). This technology allows the recapitulated TLAs to be used as host targets for viral and bacterial infectivity[27] in horizontally rotating cylindrical tissue culture vessels (RWVs)[28] that provide controlled supplies of oxygen and nutrients, with minimal turbulence and extremely low shear.[29]

These vessels rotate the wall and culture media inside at identical angular velocity, thus continuously randomizing the gravity vector and holding particles such as microcarriers and cells relatively motionless in a quiescent fluid.[29,30]

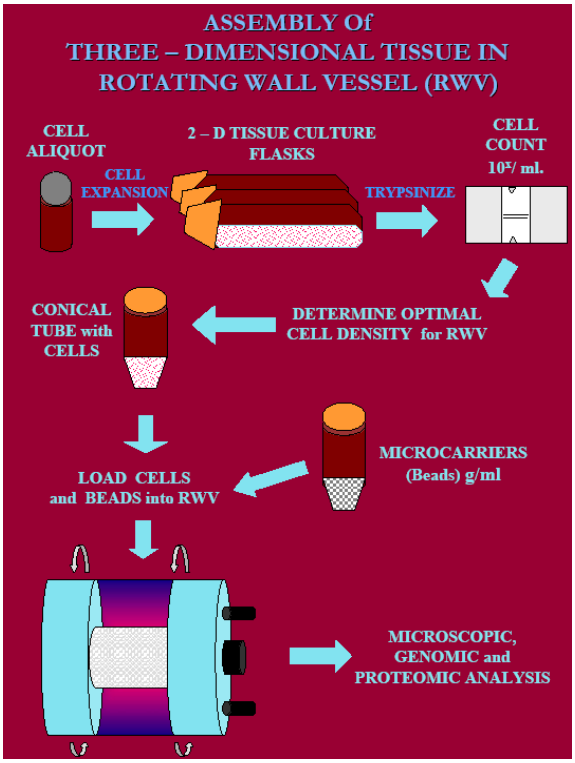

Figure 1. Tissue assembly process in a rotating cell culture system.

Table I. Human and Animal TLAs Successfully Engineered in the RWV System

NORMAL	CANCER
Bovine Cartilage (chondrocytes)[64]	Human Colon[24,25]
	Human Lung[76]
Rat Cardiomyocytes[65]	Human Ovarian[69]
	Human Prostate[67]
Human Bone (Osteoblast)[66,67]	
Human Cornea[68]	
Human Kidney [26,70]	
Human Liver[71]	
Human Lymphoid[63,72]	
Human Neural Progenitor[73,74]	
Human Renal Proximal Tubule[70]	
Human Small Intestinal Epithelial[75]	

The RWV culture system provides ease of manipulation, consistency in culture conditions, and well–differentiated TLAs that share structural and functional characteristics of the human respiratory epithelium. Culturing normal 3D epithelium configurations that are larger than 3 mm is problematic using traditional *in vitro* culture technology.[31] Thus, the factors that control proliferation and differentiation in complex human tissues are largely unknown.[32,33,34,35,36] Short-term cultures have been accomplished by a variety of methods for animal or human cells;[16,19,37,38] however, long-term growth has required sophisticated, defined culture media[39] or *in vitro* transformation to increase longevity.[40,41,42]

When combined with a solid matrix, cocultivation of epithelial and mesenchymal cells in RWVs allows cells to auto assemble into 3D tissue-like masses that we postulate fulfill four of the five basic stages of tissue regeneration and differentiation (figure 2). Here we report the successful engineering of the first *in vitro* model of the human respiratory epithelium using primary human mesenchymal bronchial-tracheal cells (HBTCs) as the foundation matrix and an adult HBE immortalized cell line BEAS-2B as the overlying component. Like the air-liquid interface model,[23] the epithelial cell organization of the TLAs improves the expression of airway epithelial characteristics, as well as cellular communication. Thus, TLAs represent a physiologically relevant model of the human respiratory epithelia that can be used in large-scale production for prolonged periods.

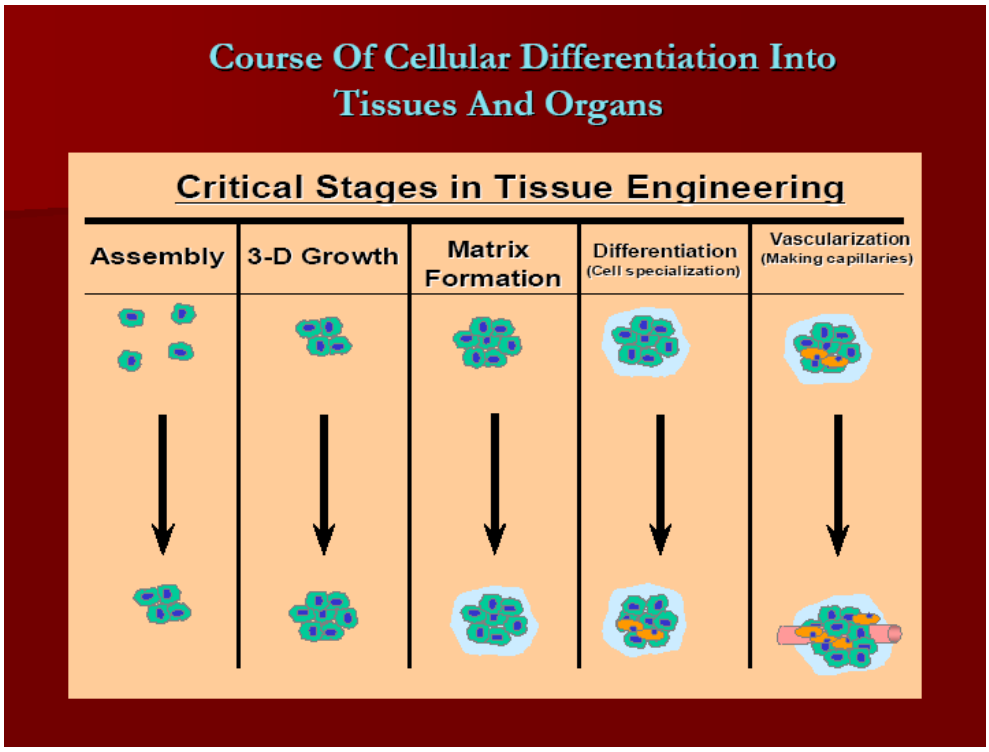

Figure 2. Five stages of tissue development and assembly.

2.0 Materials and Methods

Cell Cultures and Media

Mesenchymal cells (HBTCs) from human bronchi and tracheae were obtained from the lung mucosa of multiple tissue donors through Cambrex Biosciences (Walkersville, MD, USA). BEAS-2B epithelial cells were obtained from ATCC (Manassas, VA, USA). All were harvested and banked at Johnson Space Center's Laboratory for Disease Modelling and shown to be free of viral contamination by survey of a panel of standard adventitious viruses (e.g., human immunodeficiency virus [HIV], hepatitis, herpes) conducted by the supplier (Cambrex). Cells were initiated as monolayers in human fibronectin-coated flasks (BD Biosciences, San Jose, CA, USA) and propagated in GTSF-2 media supplemented with 10% fetal bovine serum (FBS). GTSF-2, which is a unique media formulated at Johnson Space Center,[43] was found to meet the growth requirements of the coculture system without the need for unique growth factors and most of the other complex components found in previously used culture media. GTSF-2 is a trisugar-based medium, containing glucose, galactose, and fructose supplemented with 10% FBS. All cell cultures were grown in a Forma humidified carbon dioxide (CO_2) incubator with 95% air and 5% CO_2, and constant atmosphere at a temperature of 37°C. Normal HBTC mesenchymal and BEAS-2B human lung cells were passaged as required by enzymatic dissociation with a solution of 0.1% trypsin and 0.1% EDTA for 15 minutes at 37°C. After incubation with the appropriate enzymes, the cells were centrifuged at 800 g for 10 minutes in Corning conical 50-ml centrifuge tubes. The cells were then suspended in fresh medium and diluted into T-flasks with 30 ml of fresh growth medium. BEAS-2B epithelial cells were passaged as required by dilution at a 1:4 ratio in GTSF-2 medium in T-flasks.

RWV Cultures

The RWV is a horizontally rotated transparent culture vessel with zero headspace and center oxygenation. Normal mesenchymal cell monolayers were removed from T-75 flasks by enzymatic digestion, washed once with calcium- and magnesium-free phosphate-buffered saline (CMF-PBS), and assayed for viability by trypan blue dye exclusion (Gibco). Cells were held on ice in fresh growth medium until inoculation. The primary inoculum for each coculture experiment was 2 × 105 mesenchymal (HBTC) cells/ml in a 55-ml RWV with 5 mg/ml of Cytodex-3 (Type I, collagen-coated cyclodextran) microcarriers 120 μm in diameter (Pharmacia, Piscataway, NJ, USA). Cultures were allowed to grow for a minimum of 24 to 48 hours before the medium was changed. Thereafter, fresh medium was replenished by 65% of the total vessel volume each 20 to 24 hours. BEAS-2B epithelial cells were added at 2 × 105 cells/ml on day 4. As metabolic requirements increased, fresh medium was supplemented with an additional 100 mg/dl of glucose. Coculture experiments in the RWV were grown in GTSF-2 supplemented with 10% FBS (as per references 25,26). The optimal period of culture was 15 to 20 days prior to infection with virus. Experiments were cultured for up to 40 days total including post infection (pi). Viable cocultures grown in the RWV were harvested over periods up to 21 days and prepared for various viral infectivity assays. All RWV cell cultures were grown in a Forma humidified CO_2 incubator with 94.5% air and 5.5% CO_2 providing constant atmosphere, and at a temperature of 35°C to mimic that of the nasopharyngeal epithelium.[44]

3D Cell Growth Kinetics

The cocultures were sampled over the course of the experiments, generally at 48-hour time points, to establish a cellular development profile. The parameters of glucose utilization and pH were surveyed via iStat clinical blood gas analyzer to determine the relative progress and health of the cultures and the rate of cellular growth and viability.

Normal Human Lung and 3D hLEM TLA Immunohistochemistry (IHC)

Normal human lung tissue samples and TLA tissue sections designated for histological and immunohistological staining were washed three times with gentle agitation in 1× PBS (Cellox Laboratories Inc., St. Paul, MN, USA) without magnesium and calcium for 5 minutes to remove foreign protein residues contributed by the media. The TLAs were then transferred to 50-ml polystyrene tubes and covered with 10% buffered formalin in PBS (Electron Microscopy Service, Ft. Washington, PA, USA) overnight at 4°C and washed three times in PBS. TLAs were centrifuged at low speed (1000× g) to concentrate the bead-cell assembly. Warm noble agar (1 ml) was added for additional stabilization. TLAs were embedded in paraffin-blocks by standard methods, and light sections cut at 3 to 5 um on a Micron HM315 microtome (Walldorf, Germany). All unstained sections were stored at –20°C until stained with haematoxylin and eosin (H&E) or with a panel of differential and developmental membrane receptor antibodies. The sections were deparaffinized by normal procedure,[24] antigen retrieved by protease or citrate, and blocked with a normal rabbit or mouse sera – 0.5% Tween 20 blocking solution. The primary antibody (as identified in Table II) diluted in the blocking solution was incubated on sections between 9 and 30 minutes as required, rinsed with distilled water, and incubated with anti-mouse, -goat, or -rabbit antibodies conjugated with horseradish peroxidase. The second antibody (Dako Envision System) was applied using an automated immunohistochemical stainer (Dako, Carpintaria, CA, USA). Slides were examined under a Zeiss Axioskop (Hamburg, Germany) microscope, and images were captured with a Kodak DC 290 Zoom (Rochester, NY, USA) digital camera.

Transmission Electron Microscopy

TLA transmission electron microscopy (TEM) samples were washed three times with 0.1-M sodium cacodylate buffer pH 7.4 (# 11652, Electron Microscopy Science, Port Washington, PA, USA) then fixed in a solution of 2.5% gluteraldehyde-formaldehyde in 0.1-M sodium cacodylate buffer (# 15949, Electron Microscopy Science, Fort Washington, PA, USA) – 0.3 M sucrose (Sigma, St. Louis, MO, USA) – 1% DMSO (Sigma, St. Louis, MO, USA) pH 7.4 (Electron Microscopy Science, Fort Washington, PA, USA) overnight at 4ºC. The fixed tissue was washed three times in 0.1-M sodium cacodylate buffer, pH 7.4 buffer, post-fixed stained in 0.1-M tannic acid (# 21700, Electron Microscopy Science, Port Washington, PA, USA) in 0.1-M sodium cacodylate pH 7.4 for 3 hours at room temperature. The tissue samples were washed three times in buffer, and then fixed again in 1.0-M osmium tetroxide (# 19152, Electron Microscopy Science, Port Washington, PA, USA) in cacodylate buffer pH 7.4 for 1.5 hours at room temperature. Samples were dehydrated in a series of graded ethanol (EtOH), and then were embedded in EMbed - 812 resin (# 14120, Electron Microscopy Science, Port Washington, PA, USA). Samples were sectioned at yellow-silver (700 A), mounted on Ni grids and examined under a JEOL-JEM 1010 transmission electron microscope (JEOL, USA) at 80 kV.

Scanning Electron Microscopy

Samples from the RWV cultures were taken for scanning electron microscopy (SEM) at the same times as those taken for growth kinetics and IHC. After removal from the reactor vessels, samples were washed once with CMF-PBS. The samples were suspended in a buffer containing 3% glutaraldehyde and 2% paraformaldehyde in 0.1-M cacodylate buffer at pH 7.4,[45], then rinsed for 5 minutes with cacodylate buffer three times and post-fixed with 1% osmium tetroxide (Electron Microscopy Sciences, Fort Washington, PA, USA) in cacodylate buffer for 1 hour. Samples were then rinsed three times for 5 minutes each with distilled water and treated for 10 minutes with a Millipore (Millipore Corp., Bedford, MA, USA) (0.2-μm)-filtered, saturated solution of thiocarbohydrazide (Electron Microscopy Sciences), then washed five times for 5 minutes each with distilled water and fixed with 1% buffered osmium tetroxide for 10 minutes. This last step was necessary to prevent the microcarriers from collapsing. Samples were then rinsed with distilled water three times and dehydrated with increasing concentrations of EtOH, followed by three changes in absolute methanol. After transfer to 1,1,1,3,3,3-hexamethyldisilazane (Electron Microscopy Sciences), samples were allowed to soak for 10 minutes, drained, and air-dried overnight. Dried samples were sprinkled with a thin layer of silver paint on a specimen stub, dried, coated by vacuum evaporation with platinum-palladium alloy, and then examined in the JEOL T330 SEM at an accelerating voltage of 5 to 10 kV.

Viral infection of 3D hLEM TLAs

TLAs were infected as described previously. Briefly, TLAs were inoculated with *wt*RSV A2[46,47] at a multiplicity of infection (MOI) of 0.01. Virus was obtained in cell free ampoules from American Type Culture Collection. After virus absorption at room temperature for 1 hour, monolayers and TLA cultures were washed three times with DPBS (Invitrogen, Carlsbad, CA, USA) and fed with media specified above. All air bubbles were removed from the RWV before rotation to eliminate shearing of the cells[24] and before placing in a humidified incubator with 5% CO_2 at 35.0°C. Approximately 65% of the culture media was replaced every 48 hours for both monolayer and TLA cultures. Samples were collected at days 0, 2, 4, 6, 8, and 10 for virus titration. For RSV titration, 1-mL samples of the TLA cultures were flash-frozen with 1X succinic acid-phosphate-glycine. The titer was determined by immunostaining in HEp-2 cells at 32°C as previously described.[48,49]

Immunostaining fixed RSV-infected 3D hLEM TLAs

Uninfected TLAs and TLAs (106 cells) infected with *wt*RSV A2 were fixed at different times pi, as described.[50] Briefly, paraformaldehyde (EM Grade from Electron Microscopy Sciences, cat #1570) was added to a final concentration of 4% after the TLAs were washed three times in DPBS (Cellgro cat #21-030-CV). After 1 hour, the TLAs were washed three more times with DPBS. 0.1% The TLAs were permeablized in Triton X-100 (Sigma #T9284) for 5 minutes on ice. To avoid nonspecific binding, the samples were incubated with 1% BSA for 5 minutes followed by cold water fish gelatin (Fluka #48717) in phosphate-buffered saline (PBS) at room temperature for 10 minutes. The TLAs were incubated with 0.02-M glycine (Fluka Biochemical #1050586) for 3 minutes to reduce autofluoresence. A 1:1000 dilution of RSV F (133-1H and 143-6C) and G (131-1G) monoclonal antibodies[51] was incubated for 1 hour; then the TLAs were washed five times with 1% BSA. Texas Red dye conjugated AffiniPure Goat anti-mouse IgG H + L (Jackson ImmunoResearch Laboratories #115-075-146) was diluted 1:100 and 500 μL was added to each sample for 1 hour, then washed four times with DPBS. TLAs were observed with an Olympus IX70 fluorescent microscope.

3.0 Results

RWV Cultures

Growth Kinetics of 3D hLEM TLAs

3D hLEM TLAs were produced, as illustrated in figure 1, using GTSF-2 media, and then monitored at 24-hour time points for glucose utilization and pH. Figure 3 reflects a typical metabolic profile for these cultures. These data clearly demonstrate rapid uptake of glucose by TLAs with a slight decrease in pH over the initial growth period. Together these factors indicate an increase in cellular metabolism commensurate with an increase in the size of the aggregates.

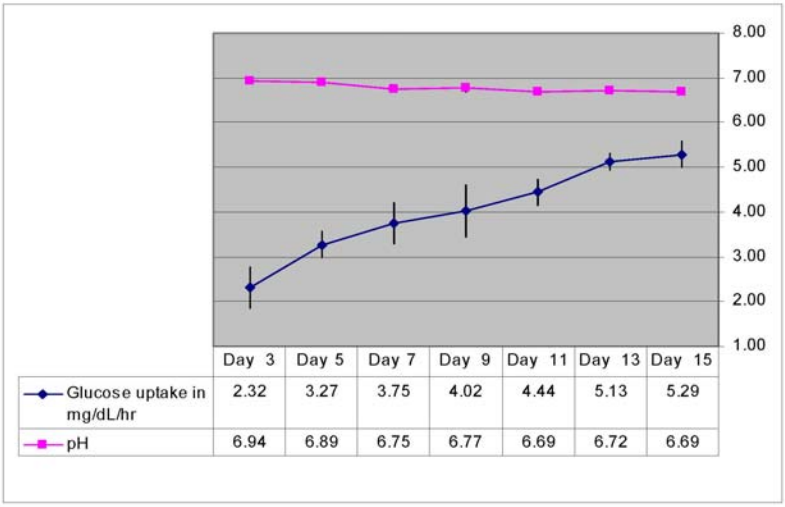

	Day 3	Day 5	Day 7	Day 9	Day 11	Day 13	Day 15
Glucose uptake in mg/dL/hr	2.32	3.27	3.75	4.02	4.44	5.13	5.29
pH	6.94	6.89	6.75	6.77	6.69	6.72	6.69

Figure 3. Glucose utilization and pH curves for a healthy 3D culture. Standard error of the mean for the pH data is < 0.08.

3D hLEM TLAs Express Specific Markers of in vivo Respiratory Epithelium (IHC)

To compare the cellular composition and differentiation state of TLAs to normal human respiratory epithelium, fixed TLAs and normal human lung sections were immunostained for epithelial-specific cell markers (figure 4, Table II). The cytokeratins (8 and 18; figure 4G, H, O, P) and Factor VIII (figure 4I, J) antibodies detect epithelial, mesenchymal, and endothelial cells, respectively.[30,40,52,53,54] Tubulin (figure 4E, F), is a cytoskeletal protein found in epithelial cells.[12,25] Endothelial markers, which are PECAM-1 (figure 4A, B) and Factor VIII (figure 4I, J), are present in subsets of precursor endothelial cells, particularly dividing cells. Basement membrane and extracellular matrix components (e.g., collagen IV; figure 4Y, Z) were also assayed to determine their expression in the TLAs. Expression of endothelial-specific and basement membrane components (Fig. 4J, Z) were frequently seen at cell-bead-aggregate interfaces. Other markers were also selected to highlight epithelial characteristics including microvilli (MV) (Villin; figure 4M, N) tight junctions (ZO-1; figure 4Q, R), and polarization (Epithelial Membrane Antigen; figure 4C, D). Expression of ICAM-1 (figure 4S, T) and cytokeratin 18 (figure 4O, P) reflects a differentiated state. Positive staining for mucin (figure 4K, L) indicates production of mucus in the tissue. Of particular interest, figure 4T, N, and F illustrates homogenous staining for cytoskeletal markers, ICAM-1, villin, and tubulin at the surfaces of most areas of the cell/microcarrier TLAs. Each of the cell-specific cellular stains applied to TLAs compared favorably with the 3D human tissue controls shown in Table III.

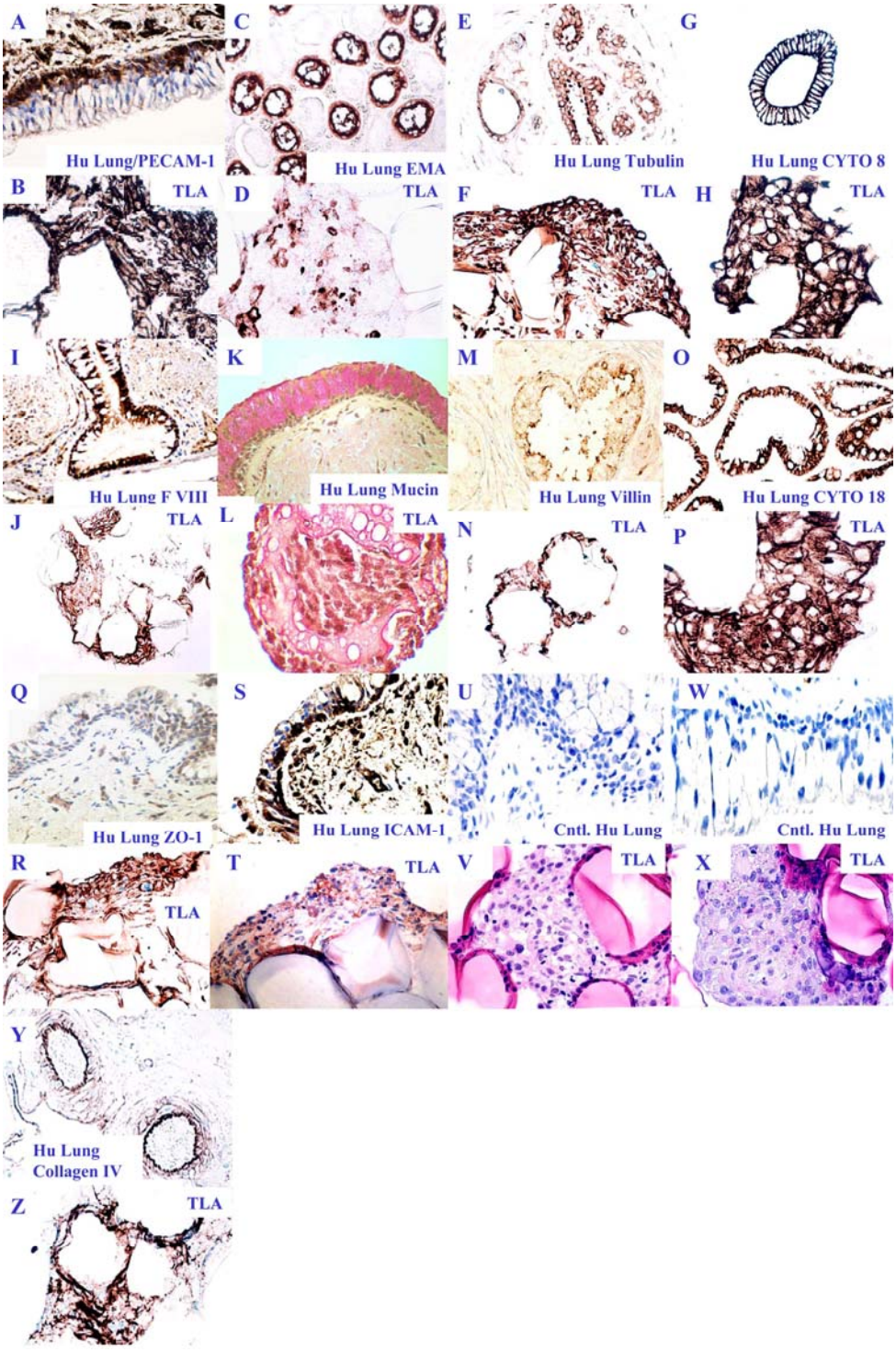

Figure 4. Comparative IHC staining of normal human lung tissue samples (A, C, E, G, I, K, M, O, Q, S, U, W, and Y) and recapitulated TLAs (B, D, F, H, J, L, N, P, R, T, V, X, and Z) formed in the rotating wall vessel. Photographs are arrayed in matched pairs showing the normal human tissue and the TLAs were stained for PECAM-1 (A and B), EMA (C and D), tubulin (E and F), cytokeratin 8 (G and H), Factor VIII (I and J), mucin (K and L), villin (M and N), cytokeratin 18 (O and P), ZO-1 (Q and R), ICAM-1 (S and T), and collagen IV (Y and Z). Sample pairs U and V and W and X are H&E histologies demonstrating human tissue organization and TLA cell density. All samples are shown at 400× magnification.

Table II. Developmental and Differential Human Immunohistochemistry Antibodies

Antibody	Manufacture	Dilution
Rabbit anti- ZO-1	Zymed, # 61-7300	1:3000
Mouse anti-Human Villin	Neomarkers, Ezrin p81/80K Cytovillin Ab-1, Clone 3C12	1:40
Mouse anti-Human Epithelial Membrane Antigen	Dako, #N1504, Clone E29	1:1500
Mouse anti-Human Endothelial Cell Membrane PECAM-1 (CD 31)	Dako, #N1596, Clone JC70A	1:500
Mucin Stain Kit	Ventana Medical Systems	NA
Mouse anti-Human Cytokeratin 8	Dako, #M0888, Clone RCK 108	predilute
Mouse anti-Human Laminin	Dako, #M0638, Clone 4C7	1:1000
Mouse anti-Swine Vimentin	Dako, #M0725, Clone V9	1:2000
Mouse anti-Human Cytokeratin 18	Dako, #N1589, Clone LP34, 34 beta E12	predilute
Rabbit anti-Human Von Willebrand Factor	Dako, # N1505	1:75
Fibronectin	Dako	1:500
Tubulin	ProMega Cat. No. #946, clone 5G8	1:1000
Collagen IV	Dako #N1536 clone CIV 22	predilute

Table III. Native Cellular Differentiation

Tissue Characterization Stains	3D/Nor Hu Lung Tissue	3D/TLA/ BEAS-2B/
ICAM-1	4+	3+
Villin	2+	3+
Tubulin	3+	4+
Cytokeratin 8	4+	3+
Cytokeratin 18	3+	4+
PECAM-1	3+	4+
ZO-1	2+	3+
EMA	4+	2+
Hu Mucin	4+	4+
VWR/ Factor VIII	4+	3+
Collagen IV	4+	4+

Slides were scored on a relative scale: 0 (no staining), 1+ (weak staining), and 2+ weak staining for 25 to 50% of the cells, 3+ indicates moderate staining for 50 to 75% of the cells, and 4+ indicates staining of 99% of the cells.

3D hLEM TLAs Display Structural Characteristics of the Human Respiratory Epithelia

TEMs of uninfected TLAs (figure 5A-F) illustrate many features of normal tissue and demonstrate that recapitulated respiratory epithelium polarized with apical and basolateral sides reinforced the IHC data. TEMs of thin sections of TLAs illustrate human respiratory epithelial characteristics including a multilayered structure punctuated by extracellular matrix and pseudo-stratified mesenchymal and epithelial layers (figure 5A, B). Multiple cell types are shown in figure 5 (C and D); the nuclei of mesenchymal cells (on bead) are elongated and the nuclei of epithelial cells are rounded. Figure 5 (E and F), the center of both micrographs demonstrates conformational data showing tight junctions (TJ) also represented by ZO-1 IHC staining. MV, stained by villin and tubulin on IHC, can be seen in figure 5F. Further successful villin and tubulin reflects the presence of MV as demonstrated in figure 5F.

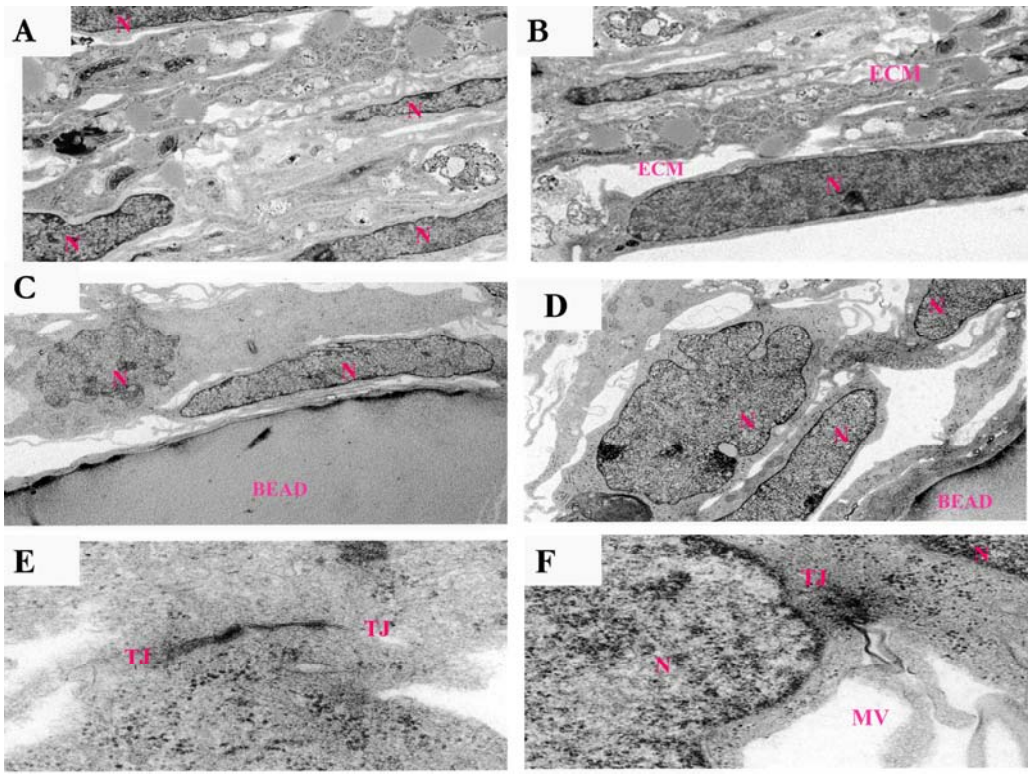

Figure 5. TEMs of uninfected TLAs, A and B (mag. × 7,500) show TLAs that are multilayered (six or seven layers of long thin cells with dark nuclei) and demonstrate extracellular matrix material between the cells; C and D (mag. × 7,500) demonstrate both mesenchymal and epithelial cells (oval and elongated nuclei) lying close to the bead surface; E and F (mag × 50,000) demonstrate cellular TJ and MV are visible in F.

3D hLEM TLAs are Susceptible to Infection by Respiratory Viruses

Scanning Electron Microscopy

TLAs were infected with *wt*RSV A2 at an MOI of 0.01 at 35.0°C, which is the upper temperature of the human respiratory epithelium. TLA samples were collected at intervals across the initial growth experiment (figure 6A, B uninfected) and pi (figure 6C-F) and were prepared for SEM as stated previously. Photomicrographs taken of day 2 through 12 cocultures pi showed viral presence and cellular damage (figure 6C, D). Figure 6E demonstrates cell surface damage analogous to pockmarks at 8 days pi. In figure 6F, 12 days pi, an insert of budding virus (BV) is visible. Samples harvested at approximately 12 days of culture contained small microcarrier bead packs that were totally engulfed in proliferating TLA epithelium despite viral infection (Fig. 6E, F). Additionally, at 20 days, large proliferating masses of TLAs (>3.5mm) were evident, growing on the microcarrier bead packs pi.

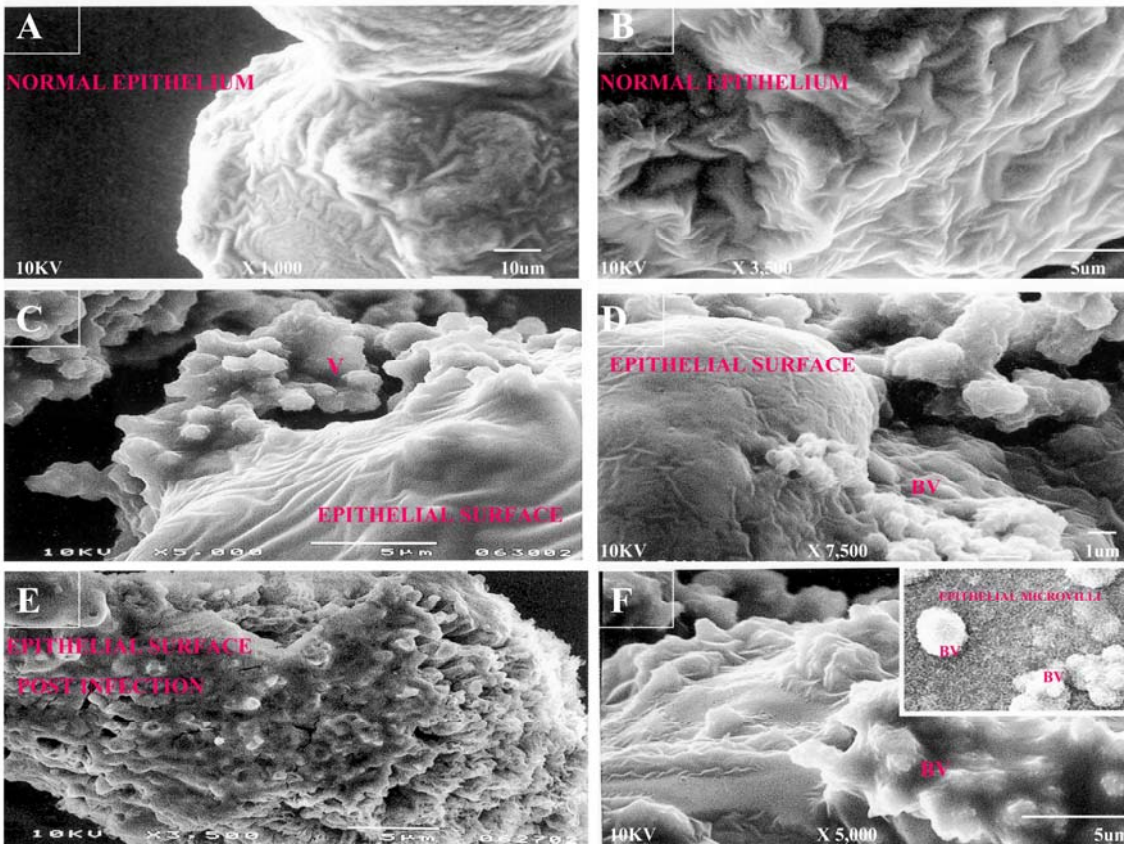

Figure 6. SEMs of TLAs infected with *wt*RSV A2, A and B demonstrate healthy noninfected (smooth) epithelium; C and D demonstrate clusters of BV atop the epithelium on day 2 and 4 pi; E illustrates the result of viral infection of the epithelial layer on day 8 pi. Notice the pockmarked appearance of the once-smooth epithelium. F demonstrates an inset of BV masses from an infected epithelium on day 12 pi.

Transmission Electron Microscopy

TLAs, as previously stated, were infected. Figure 7A-F illustrates the time course of infection into the 3D hLEM TLAs from 0 to 12 days, respectively. TEMs of all TLAs subjected to virus demonstrated infection beginning as early as 1 hour pi, figure 7B, and continuing through day 12 pi figure 7F. Viral nucleocapsids (VNCs) were found to locate throughout the cells and in the perinuclear regions (figure 7B, E and F) and were overtly apparent in all RSV-infected TLAs. Mature virus particles are formed when VNCs bud from the cell membrane containing the viral glycoproteins; thus BV was present beginning at day 2 (figure 7C) and day 4 (figure 7D) and continuing throughout the course of the infection.

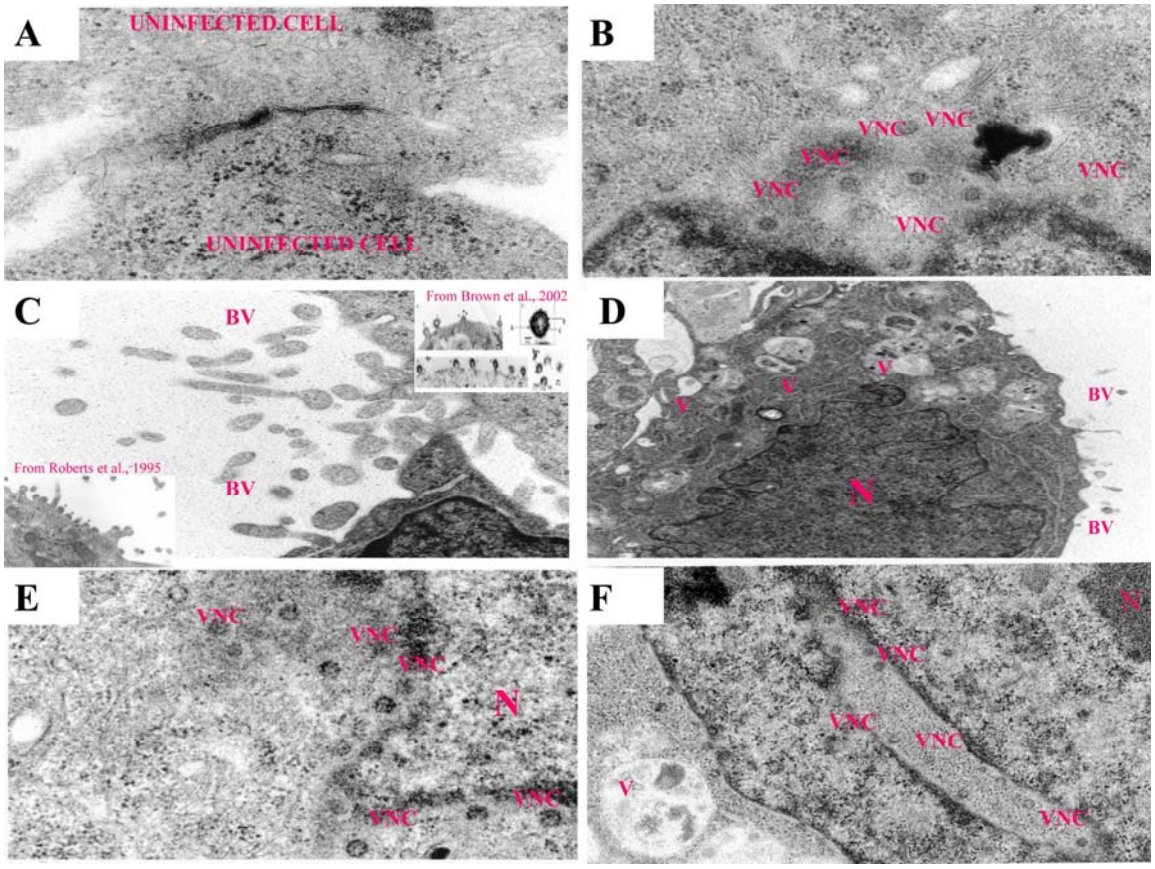

Figure 7. TEMs of *wt*RSV A2-infected TLA epithelium. A is an uninfected micrograph showing a TJ between cells at time zero. B demonstrates VNC present in the perinuclear area of the cell at 1 hour pi. Both A and B shown at mag. × 50,000. C (mag. × 50,000) and D (mag. × 12,000) illustrate the presence of BV at 2 and 4 days pi, respectively, and vacuoles (Vs) in D at day 4 pi. E (mag. × 50,000) and F (mag. × 25,000) show VNC present in the cells at days 8 and 12 pi, respectively.

Viral Protein and Titer Data

Photographs of fluorescently stained TLAs, which are specific for RSV glycoprotein that increased in concentration (days 2 to 10), are shown in figure 8A-D. Figure 9 illustrates viral growth kinetics up to day 20 pi with *wt*RSV A2. As illustrated, *wt*RSV A2 replicated well in TLAs with peak replication occurring on day 10 (approximately 7 log10 particle forming units per mL).

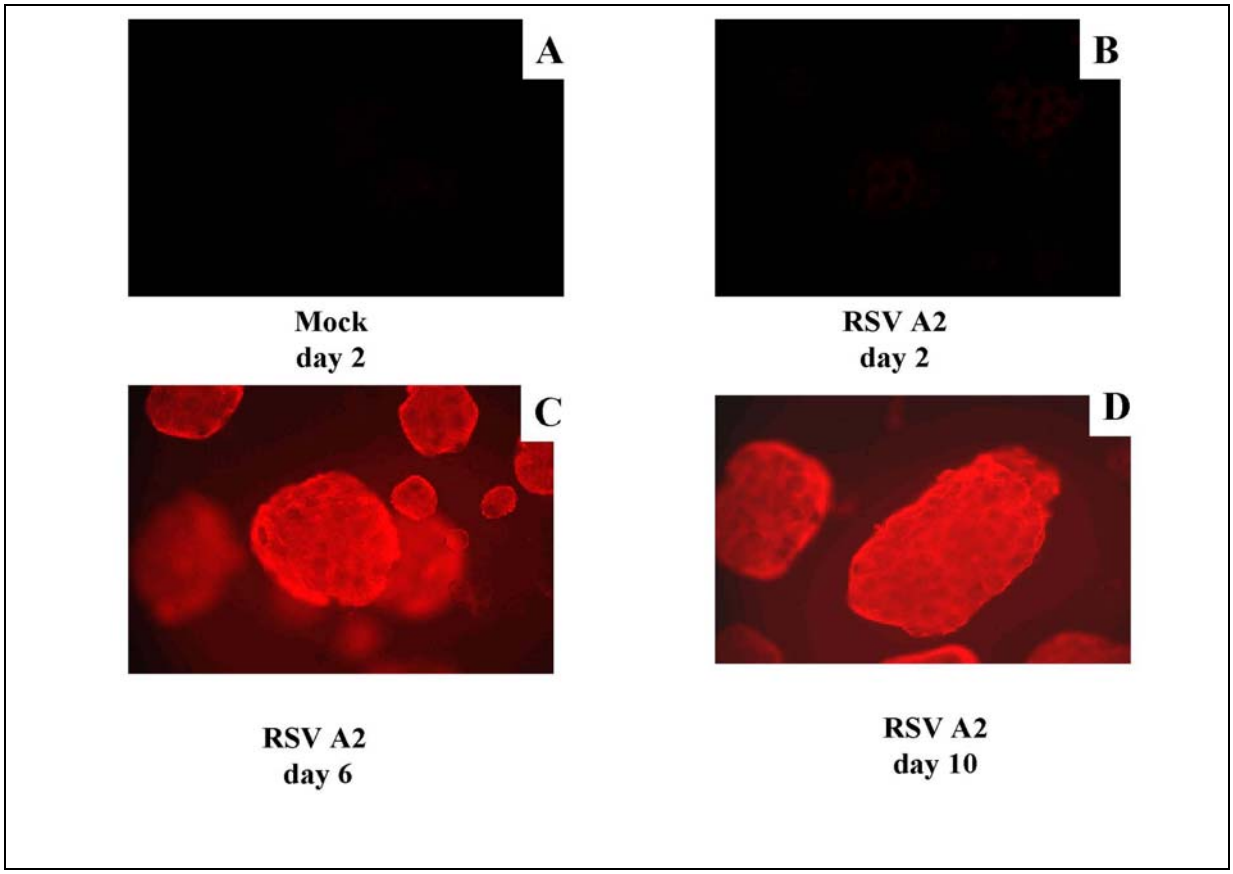

Figure 8. The increase in expression of RSV F and G glycoproteins from day 2 to 10 pi.

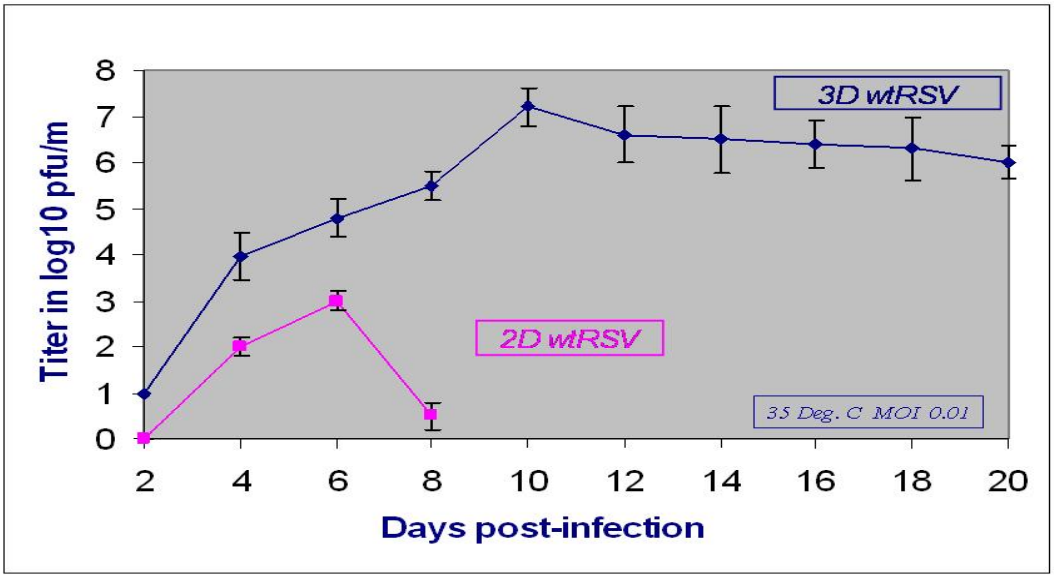

Figure 9. Growth kinetics of *wt*RSV A2 in recapitulated TLAs up to day 20.

4.0 Discussion

The data presented constitute a major advance in the construction of a functionally accurate, large-scale > 3mm, 3D *in vitro* tissue model of the human airway. The recapitulation of large TLAs that express differentiated epithelial and mesenchymal cell markers offers a multitude of possibilities for cell biological investigations. Functional epithelial cell brush borders with extracellular matrix and basal lamina components represent ordering of tissue and cellular polarity nurtured by the molecular conditions and physical orientations of the culture system. These data, which are confirmed in figures 4 (IHC) and 5 (TEM), represent concomitant cellular differentiation marker expression and architectural ordering when compared to normal human tissue. Additionally, this 3D model demonstrates a significantly diminished requirement for complex culture media in the RWV culture system. The growth of mesenchymal and epithelial cells in the absence of complex media infers specific cell-cell interactions and the production of the paracrine and autocrine factors essential to the growth, development, and differentiation of these fragile tissues. The nature of these factors, cytokines, and cellular interactions and their roles at the molecular and genetic levels are a subject for further investigations.

The role of basement membranes and extracellular matrix and their relationship to epithelio-mesenchymal development and differentiation and infectivity are the subject of considerable research. Studies indicate, for example, that the stromal component exerts a driving influence over developing intestinal mucosa,[55,56,57,58] have shown that only organ-specific mesenchyme will produce differentiation in epithelium from a given organ site, and that embryonic mesenchyme of the same age but from different organs is ineffective.[59,60] Finally, a recent publication demonstrated that 3D aggregates derived from an alveolar epithelial tumor cell line (A549) were used as targets for bacterial infection.[11] These aggregates, while far superior to 2D cultures (as demonstrated in the text), lacked some of the functional and structural characteristics we report with TLA cocultures. Additionally, the air liquid interface (ALI) models (reported by reference 61) show cellular differentiation, basolateral orientation, and cilia, but lack the fidelity of *in vivo* tissues as the ALI tissue density is approximately 3 to 5 cell layers versus dozens of cell layers achieved in TLAs.

The TLA model of human lung embodies most aspects of differentiation and cellular organization observed in other *in vitro* and *in vivo* cell and organ models, including the presence of MV. Primary distinctions for this model are: (i) the overall scale of the model > 3.5mm diameter inclusive of cellular density translating to in excess of 20 cell layers, a distinct benefit for clinical and industrial utility; (ii) the ability to culture epithelium for periods in excess of 35 days without loss of functional cell markers; (iii) the ability to maintain viral production for 20 days pi and cellular repair while maintaining the model; and (iv) the ability of the system to respond to extensive analyses and manipulations without the termination of a given experiment. Future experiments will use genomic and proteomics technologies to clarify and characterize the potential of this new model system. Of particular interest will be regulation of unique cytoskeletal proteins such as villin, functional markers such as tubulin, ZO-1, EMA, ICAM-1, myriad inflammatory response modifiers, and other markers that may be represented more accurately by large-scale 3D modeling.

The molecular basis of inflammatory responses and pathogenesis of the human lung to many airborne and blood-borne infections may be investigated with the advent of this new technology. Further, clinical response and treatment of diseases may be accomplished more efficiently as a result of rapid vaccine development. Analogous to the data presented for RSV, HIV is shown to replicate in human 3D

lymphoid tissues and complex epithelium that are maintained in the RWV; thus, immunodeficiency virus-host interactions in the RWV culture system are possible.[41,62,63] This hypothesis is being investigated at the National Institutes of Health. On this basis, we propose the potential broad application of this culture model may lead to advances in understanding the developing human lung, the potential treatment of myriad clinical conditions, and advances in regenerative medicine.

5.0 Acknowledgments

This work has been supported in part by Wyeth Vaccine Discovery and NASA's Human Health and Countermeasures Division, Biological Systems Office Contract No. NAS 9-17720, and NASA RAN 72R 959-88-0046-05 (FRN 100000320). The authors would like to acknowledge the efforts of Miguel Suderman for his expertise in the preparation of the SEMs depicted in this manuscript. In addition, we wish to thank Dr. H.Q. Wang of the University of Texas Medical Branch, Department of Pathology, in Galveston, Texas, for his guidance and participation in IHC analyses. Finally, we offer great appreciation to Ms. Julia Land for her assistance in the preparation of this manuscript.

6.0 References

1. Hiemstra, P.S. and Bals, R. Series Introduction: innate host defense of the respiratory epithelium. J. Leukocyte Biol. **75**, 3-4 2004.

2. Knight, D.A. and Holgate, S.T. The airway epithelium: structural and functional properties in health and disease. Respirology **8,** 432-446 2003.

3. Gibson, M.C. and Perrimon, N. Apicobasal polarization: epithelial form and function. Curr. Opin. Cell Biol. **15**, 747-752 2003.

4. Bals, R. and Hiemstra, P.S. Innate immunity in the lung: how epithelial cells fight against respiratory pathogens. Eur. Respir. J. **23**, 327-333, 2004.

5. Cotran, R., Kumar, V., and Collins, T. Robbins Infectious Diseases, Edn. 6th p. 347 (WB Saunders Company, Philadelphia; 1999).

6. Garofola, R. P. and Haeberle, H. Epithelial regulation of innate immunity to respiratory syncytial virus. Am. J. Respir. Cell Mol. Biol. **23**, 581-85, 2000.

7. Polito, A. J. and Proud, D. Epithelial cells as regulators of airway inflammation. J. Allergy Clin. Immunol. **102**, 714-8. 1998.

8. Ke, Y. et al. Human bronchial epithelial cells with integrated SV40 virus T antigen genes retain the ability to undergo squamous differentiation. Differentiation **38**, 60-66 1988.

9. Stoner, G.D., Katoh, Y., Foidart, J.M., Myers, G.A. and Harris, C.C. Identification and culture of human bronchial epithelial cells. Methods Cell Biol. 21A, 15-35 1980.

10. Wu, R., Sato, G.H., and Whitcutt, M.J. Developing differentiated epithelial cell cultures: airway epithelial cells. Fundam. Appl. Toxicol. **6**, 580-590 1986.

11. Carterson, A.J., et al. A549 lung epithelial cells grown as three-dimensional aggregates: Alternative tissue culture model for *Pseudomonas aeruginosa* pathogenesis. Infection and Immunity **73** (2), 1129-1140, 2005.

12. Gray, T.E., Guzman, K., Davis, C.W., Abdullah, L.H., and Nettesheim, P. Mucociliary differentiation of serially passaged normal human tracheobronchial epithelial cells. Am. J. Respir. Cell Mol. Biol. **14**, 104-112 1996.

13. Wright, P.F. et al. Growth of respiratory syncytial virus in primary epithelial cells from the human respiratory tract. J. Virology **79** (13) 8651-8654, 2005.

14. Adler, K.B. and Li, Y. Airway epithelium and mucus. Intracellular signaling pathways for gene expression and secretion. Am. J. Respir. Cell. Mol. Biol. **25**, 397-400, 2001.

15. Whiticutt, M.J., Adler, K.B., and Wu, R. A biphasic chamber system for maintaining polarity of differentiation of cultured respiratory tract epithelial cells. In Vitro Cellular and Developmental Biology **24**(5), 420-428 1988.

16. Fukamachi, H., Mizuno, T., and Kim, Y.S. Morphogenesis of human colon cancer cells with fetal rat mesenchymes in organ culture. Experientia **42**, 312–315, 1986.

17. Wiens, D., Park, C.S., and Stockdale, F.E. Milk protein expression and ductal morphogenesis in the mammary gland in vitro: Hormone-dependent and -independent phases of adipocyte-mammary epithelial cell interaction. Dev. Biol. **120**, 245–258, 1987.

18. Sutherland, R.M. Cell and environment interactions in tumor microregions: The multicell spheroid model. Science **240**, 177184, 1988.

19. Kaye, G.I., Pascal, R.R., and Lane, N. The colonic pericryptal fibroblast sheath: Replication, migration, and cyto-differentiation of a mesenchymal cell system in adult tissue. 3. Replication and differentiation in human hyperplastic and adenomatous polyps. Gastroenterology **60**, 515–536, 1971.

20. Buset M., Winawer, S., and Friedman, E. Defining conditions to promote the attachment of adult human colonic epithelial cells. In Vitro **23**, 403–412, 1987.

21. Daneker, G.W., Jr, Mercurio A.M., Guerra, L., Wolf, B., Salen, R.R., Bagli, D.J., and Steele, G.D. Laminin expression in colorectal carcinomas varying in degree of differentiation. Arch. Surg. **122**,1470-1474, 1987.

22. Durban, E. Mouse submandibular salivary epithelial cell growth and differentiation in long term culture: Influence of the extracellular matrix. In Vitro Cellular & Dev. Biol. **26**, 33–43, 1990.

23. O'Brien, L.E., Zegers, M.M.P., and Mostov, K.E. Building epithelial structure: insights from three-dimensional culture models. Nature Reviews **3**:531-537 2002.

24. Goodwin T.J., Jessup, J.M., Sams, C.F., and Wolf, D.A. In Vitro Three Dimensional Modeling. Annual report of Johnson Space Center Research and Technology, pp156–157, 1988.

25. Goodwin, T.J., Jessup, J.M., and Wolf, D.A., Morphologic differentiation of colon carcinoma cell lines HT-29 and HT-29KM in rotating wall vessels. In Vitro Cellular & Dev. Biol. **28A**, 47–60, 1992.

26. Goodwin, T.J., Prewett, T.L., Wolf, D.A., and Spaulding, G.F. Reduced shear stress: a major component in the ability of mammalian tissues to form three-dimensional assemblies in simulated microgravity. J. Cell Biochem. **51**, 301-311 1993.

27. Goodwin, T.J., et al. Pathogen Propagation in Cultured Three-Dimensional Tissue Masses U.S. Patent, 6,117,674, 2000.

28. Schwarz, R.P., Wolf, D.A., and Trinh, T. Rotating cell culture vessel. U.S. Patent No. 5,026,650, 1991.

29. Schwarz, R.P., Goodwin, T.J, and Wolf, D.A. Cell culture for three dimensional modeling in rotating-wall vessels: An application of simulated microgravity. J. Tiss. Cult. Meth. **14**, 51–58, 1992.

30. Tsao, Y.D., Goodwin, T.J., Wolf, D.A., and Spaulding, G.F. Responses of gravity level variations on the NASA/JSC bioreactor system. The Physiologist **35**, 549–550, 1992.

31. Chantret, I., Barbat, A., Dussaulx, E., Brattain, M.G., and Zweibaum, A. Epithelial polarity, villin expression, and enterocytic differentiation of cultured human colon carcinoma cells: A survey of twenty cell lines. Cancer Res. **48**, 1936–1942, 1988.

32. Corps, A.N. and Brown, K.D. Stimulation of intestinal epithelial cell proliferation in culture by growth factors in human and ruminant mammary secretions. J. Endocrinol. **113**, 285–290, 1987.

33. Pyke, K.W. and Gogerly, R.L. Murine fetal colon in vitro: Assays for growth factors. Differentiation **29**, 56–92, 1985.

34. O'Loughlin, E.V., Chung, M., Hollenberg, M., Hayden, J., Zahavi, I., and Gall, D.G. Effect of epidermal growth factor on ontogeny of the gastrointestinal tract. Am. J. Physiol. **249**, 674–678, 1985.

35. Blay, J. and Brown K.D. Epidermal growth factor promotes the chemotactic migration of cultured rat intestinal epithelial cells. J. Cell Physiol. **124**,107–112, 1985.

36. Blay, J. and Brown K.D. Functional receptors for epidermal growth factor in an epithelial-cell line derived from the rat HBTC/BEAS-2B TLA. Biochem. J. **225,** 85–94, 1985.

37. Kleinman, D., Sharon, Y., Sarov, I., and Inlet, V. Human endometrium in cell culture: A new method for culturing human endometrium as separate epithelial and stromal components. Arch. Gynecol. **234**, 103–112, 1983.

38. Reid, L.M. and Jefferson, D.M. Culturing hepatocytes and other differentiated cells. Hepatology. **4**, 548–559, 1987.

39. Moyer, M.P. Mechanisms of tumor initiation and progression. Perspect. Gen. Surg. **1**,71–91, 1990.

40. Moyer, M.P., Dixon, P.S., Culpepper, A.L., and Aust, J.B. The in vitro propagation and characterization of normal, preneoplastic and neoplastic colonic epithelial cells. In: Moyer, M.P., and Poste, G.H., Eds. Colon Cancer Cells. San Diego: Academic Press, pp85–136, 1990.

41. Moyer, M.P. Methods for propagation and characterization of human GI and other cells for study of HIV. J. Tiss. Cult. Meth. **13**, 107–116, 1991.

42. Shamsuddin, A. Colon organ culture as a model for carcinogenesis. In: Moyer, M.P., Poste, G.H., Eds. Colon Cancer Cells. San Diego: Academic Press, pp137–153, 1990.

43. Goodwin, T.J. Media compositions for three-dimensional mammalian tissue growth under microgravity culture conditions. U.S. Patent No.5,846,80, 1998.

44. McFadden, E. R. et al. Thermal mapping of the airways in humans. J Appl Physiol **58**:564-70, 1985.

45. Luna, L.G., (Ed.). Histologic staining methods. In: American Registry of Pathology, 3rd ed. New York: Armed Forces Institute of Pathology, 1968.

46. Lewis, et al. A syncytial virus associated with epidemic disease of the lower respiratory tract in infants and young children. Med. J. Aust. 2, 932-933, 1961.

47. Belshe, R.B. and Hissom, F.K. Cold adaptation of parainfluenza virus type 3: induction of three phenotypic markers. J. Med. Virol. **10** (4), 235-42. 1982.

48. Randolph, V.B., et al. Attenuated temperature-sensitive respiratory syncytial virus mutants generated by cold adaptation. Virus Res, **33**, 241-259 1994.

49. Karron, R.A., et al. A live human parainfluenza type 3 virus vaccine is attenuated and immunogenic in healthy infants and children. J. Infect. Dis. **172**, 1445-1450 1995.

50. Cheutin, T., O'Donohue, M.F., Bearchia, A., Klein, C., Kaplan, H., and Ploton, D. Three-dimensional organization of pKi-67: A comparative fluorescence and electron tomography study using fluoronanogold. The Journal of Histochemistry & Cytochemistry **51**(11),1411-1423, 2003.

51. Anderson, L.J., Bingham, P., and Hierholzer, J.C. Neutralization of respiratory syncytial virus by individual and mixtures of F and G protein monoclonal antibodies. J. Virol. **62**, 4232-8, 1988.

52. Woodcock-Mitchell, J., Eichman, R., Nelson, W.G., and Sun, T. Immunolocalization of keratin polypeptides in human epidermis using monoclonal antibodies. J. Cell Biol. **95**, 580–588, 1982.

53. Vogel, A.M. and Gown, A.M. Monoclonal antibodies to intermediate filament proteins. In: Shay, J.W., Ed. Cell and Muscle Motility. New York: Plenum Publishing, Vol **5**: pp379–402, 1984.

54. Shima, M., Yoshioka, A., Nakai, H., Tanaka, I., Fujiwara, T., Terada, S., Imai, S., and Fukui, H. Factor VIII polypeptide specificity of monoclonal anti-factor VIII antibodies. Br. J. Haematol. **70**,63–69, 1988.

55. Haffen, K., Ceding, M., and Acumen, P. Mesenchyme-dependant differentiation of epithelial progenitor cells in the gut. J. Pediatr. Gastroenterol. Nutr. **6**,14–23, 1987

56. Kedinger, M., Simon-Assman, P.M., Lacrois, B., Marxer, A., Hauri, H.P., and Haffen, K. Fetal gut mesenchyme induces differentiation of cultures intestinal endodermal and crypt cells. Dev. Biol. **113**, 474483, 1986.

57. Kedinger, M., Haffen, K., and Simon-Assman, P. Intestinal tissue and cell cultures. Differentiation **36**, 71–85, 1987.

58. Stallmach, A., Hahn, U., Merker, H.J., Hahn, E.G., Rieken, E.O. Differentiation of rat intestinal epithelial cells is induced by organotypic mesenchymal cells in vitro. Gut **30**, 959–970, 1989.

59. Quaroni, A. Crypt cell development in newborn rat HBTC/BEAS-2B TLA. J. Cell Biol. **100**, 1601–1610, 1985.

60. Quaroni, A. Development of fetal rat intestine in organ and monolayer culture. J. Cell Biol. **100**, 1611–1622, 1985.

61. Zhang, L., Bukreyev, A., Thompson, C.I., Watson, B., Peeples, M.E., Collins, P.L., Pickles, R.J. Infection of ciliated cells by human parainfluenza virus type 3 in an in vitro model of human airway epithelium. J. Virology **79,** 1113-1124, 2005.

62. Moyer, M.P., Hout, R.I., Ramirez, A., Jr, Joe S, Meltzer, M.S., and Gendelman, H.E. Infection of human gastrointestinal cells by HIV-1. AIDS Res. Hum. Retroviruses **6**,1409–1415, 1990.

63. Margolis, L.B. et al. Lymphocyte trafficking and HIV infection of human lymphoid tissue in a rotating wall vessel bioreactor. AIDS Research and Human Retroviruses. **13** (16)1411-1420, 1997.

64. Baker, T.L. and Goodwin, T.J. Three-dimensional culture of bovine chrondrocytes in rotating-wall vessels. In Vitro Cellular & Dev. Biol. **33** (5),358-365, 1997.

65. Bursac, N., et al. Cultivation in rotating bioreactors promotes maintenance of cardiac myocyte electrophysiology and molecular properties. Tissue Eng**. 9** (6), 1243-53, 2003.

66. Klement, B.J., Young, Q.M., George, B.J., and Nokkaew, M. Skeletal Tissue Growth, Differentiation, and Mineralization in the NASA Rotating Wall Vessel**.** Bone **34**: (3), 487-498, 2004.

67. Wang, R., et al. Three-dimensional co-culture models to study prostate cancer growth, progression, and metastasis to bone . Review: Seminars in Cancer Biology, (15) 353-354, 2005 .

68. O'Connor, K.C., et al**.** Three Dimensional Optic Tissue Culture and Process, U.S. Patent, 5,962,324, 1999.

69. Goodwin, T.J., Prewett, T.L., Spaulding, G.F., and Becker, J.L. Three-dimensional culture of a mixed mullerian tumor of the ovary: expression of in vivo characteristics. In Vitro Cellular & Dev. Biol., **33** (5),366-374, 1997.

70. Hammond, T.G., et al. Gene Expression in Space. Nature Medicine. Vol. **5**, 4. 1999.

71. Yoffe, B., et al. Cultures of human liver cells in simulated microgravity environment. Adv. Space Res. Vol. **24**, 6 829-836,1999.

72. Pellis, N.R., et al. Changes in Gravity Inhibit Lymphocyte Locomotion through Type I Collagen . In Vitro Cell Dev. Biol. Anim. **33,** 398-405, 1997.

73. Goodwin, T.J. Physiological and Molecular Genetic Effects of Time-Varying Electromagnetic Fields on Human Neuronal Cells, NASA Technical Paper-2003-212054, September 2003.

74. Goodwin, T.J., McCarthy, M.A., and Dennis, R.G. Physiological And Molecular Genetic Effects Of Time Varying Electromagnetic Fields (TVEMF) On Human Neuronal Cells. Medicine and Science in Sports and Exercise, Vol**. 37**:5 Suppl. 2005.

75. Goodwin, T.J., Schroeder, W.F., Wolf, D.A., and Moyer, M.P. Coculture of Normal Human Small Intestine Cells in a Rotating-Wall Vessel Culture System. Proceedings of the Society for Experimental Biology and Medicine Vol. 202, 1993.

76. Vertrees, R.A., et al. Synergistic interaction of hyperthermia and gemcitabine in lung cancer, Cancer Biology and Therapy, 1:4 (10) Oct. 2005.

REPORT DOCUMENTATION PAGE

Form Approved
OMB No. 0704-0188

1. AGENCY USE ONLY *(Leave Blank)*	2. REPORT DATE	3. REPORT TYPE AND DATES COVERED
	March 2008	NASA Technical Paper

4. TITLE AND SUBTITLE
Three-Dimensionally Engineered Normal Human Lung Tissue-Like Assemblies: Target Tissues for Human Respiratory Viral Infections

5. FUNDING NUMBERS

6. AUTHOR(S)
Thomas J. Goodwin, NASA Johnson Space Center, Houston, TX 77058
M. McCarthy,Universities Space Research Association, Houston, TX 77058
Y-H. Lin, A.M Deatly, Vaccines Discovery, Wyeth Research, Pearl River, New York 10965

7. PERFORMING ORGANIZATION NAME(S) AND ADDRESS(ES)
Lyndon B. Johnson Space Center
Houston, Texas 77058

8. PERFORMING ORGANIZATION REPORT NUMBERS
S-1022

9. SPONSORING/MONITORING AGENCY NAME(S) AND ADDRESS(ES)
National Aeronautics and Space Administration
Washington, DC 20546-0001

10. SPONSORING/MONITORING AGENCY REPORT NUMBER
TP-2008-214771

11. SUPPLEMENTARY NOTES

12a. DISTRIBUTION/AVAILABILITY STATEMENT
Available from the NASA Center for AeroSpace Information (CASI)
7115 Standard
Hanover, MD 21076-1320 Category: 52

12b. DISTRIBUTION CODE

13. ABSTRACT *(Maximum 200 words)*

In vitro three-dimensional (3D) human lung epithelio-mesenchymal tissue-like assemblies (3D hLEM TLAs), from this point forward referred to as TLAs, were engineered in rotating wall vessel technology to mimic the characteristics of in vivo tissues, thus providing a tool to study human respiratory viruses and host cell and viral interactions. The TLAs were bioengineered onto collagen-coated cyclodextran microcarriers using primary human mesenchymal bronchial-tracheal cells as the foundation matrix and an adult human bronchial epithelial immortalized cell line as the overlying component. The resulting TLAs share significant characteristics with in vivo human respiratory epithelium including polarization, tight junctions, desmosomes, and microvilli. The presence of tissue-like differentiation markers including villin, keratins, and specific lung epithelium markers, as well as the production of tissue mucin, further confirm that these TLAs differentiated into tissues functionally similar to in vivo tissues. Increasing virus titers for human respiratory syncytial virus and the detection of membrane bound glycoproteins over time confirm productive infection with the virus. Therefore, we assert TLAs mimic aspects of the human respiratory epithelium and provide a unique capability to study the interactions of respiratory viruses and their primary target tissue independent of the host's immune system.

14. SUBJECT TERMS	15. NUMBER OF PAGES	16. PRICE CODE
epithelium, respiratory, cells, cell culturing, cultured cells, in vitro methods and tests	34	

17. SECURITY CLASSIFICATION OF REPORT	18. SECURITY CLASSIFICATION OF THIS PAGE	19. SECURITY CLASSIFICATION OF ABSTRACT	20. LIMITATION OF ABSTRACT
Unclassified	Unclassified	Unclassified	Unlimited